

# Transgranular fracture in low temperature brittle fracture of high nitrogen austenitic steel

Shiyong Liu · Deyi Liu · Shicheng Liu

Received: 25 May 2006 / Accepted: 8 February 2007 / Published online: 18 May 2007  
© Springer Science+Business Media, LLC 2007

**Abstract** Morphological features of transgranular fracture facets in low temperature brittle fracture of 18Cr–18Mn–0.7N high nitrogen austenitic steel have been studied by means of scanning electron microscopy and their formation mechanisms have been discussed. The transgranular fracture facets are fairly coarse compared with intergranular fracture facets and annealing twin boundary fracture facets. There are parallel steps and river patterns on the facets. Dual-surface observation indicated that these patterns are parallel to {111} planes and of strict crystallographic features. Microstructure observation shows that there are a lot of planar deformation structures formed prior to low temperature transgranular fracture. Transgranular fracture originates from microcracks formed at the intersections of the deformation structures on different {111} planes. These microcracks propagate toward adjacent microcracks on different {111} planes, forming transgranular fracture facets with steps and river patterns.

## Introduction

Low carbon steels having BCC crystal structures exhibit ductile-to-brittle transition with decreasing temperature. Accompanying the ductile-to-brittle transition, appearance

of the fracture surface changes from dimple to cleavage rupture along specific crystallographic planes. Cleavage steps and river patterns can be observed on the cleavage surface [1]. It is generally believed that there is no ductile-to-brittle transition for FCC austenitic stainless steel. Nevertheless, brittle fracture at low temperature in high strength and high nitrogen austenitic steels has recently been reported [2–10]. To ascertain their mechanism of fracture at low temperature, some researchers examined the fracture and found smooth and flat facets that develop along {111} planes with three sets of linear patterns intersecting each other at 60°C on them. This type of fracture facet propagates along specific crystallographic planes, which is one of characteristics of cleavage fracture. However, no cleavage steps and river patterns were observed on the facet [2, 3]. Hence, this type of fracture facet was termed as transgranular cleavage-like facet. Still, mechanism of low temperature brittle fracture in high nitrogen austenitic steel as well as mechanism of formation of the facet remains unknown.

Recently, authors of this paper examined the fracture surface and its adjacent side surface of an 18Cr–18Mn–0.7N austenitic steel by a dual-surface observation technique under SEM, and exemplified that there exist three fracture modes in low temperature brittle fracture of the steel: annealing twin boundary fracture, intergranular fracture and transgranular fracture [11, 12]. Conclusive evidences show that the so-called transgranular cleavage-like facet in early literatures is virtually annealing twin boundary facet [11–14], not a consequence of transgranular fracture. The real transgranular facet is very coarse [11, 12]. Further detailed observation revealed that there are still steps and river patterns on the transgranular fracture facet of low temperature brittle fracture in the FCC high nitrogen austenitic steel, just similar to the transgranular

---

S. Liu (✉)  
Electromechanics and Materials Engineering College, Dalian  
Maritime University, Dalian 116026, China  
e-mail: shiyong@newmail.dlmu.edu.cn

D. Liu · S. Liu  
College of Materials Science and Engineering, Dalian Jiaotong  
University, Dalian 116028, China

cleavage fracture facet in BCC metals. It is the particularity of deformation structure and transgranular crack formation in the FCC high nitrogen austenitic steel that makes the steps and river patterns on its transgranular fracture facets have their own distinctive crystallographic features. This paper deals with observation of the features and analysis on the formation mechanisms of transgranular fracture facet in low temperature brittle fracture of high nitrogen austenitic steel.

### Experimental material and procedure

The high nitrogen austenitic steel used in the present work is composed of 0.048C, 19.33Cr, 19.40Mn, 0.70N, 0.42Si, 0.029P, 0.008S, 0.27Ni (wt%), and balance Fe. It was melted and cast in vacuum. The ingot was then hot forged and cold-rolled into sheets 2 mm and 10 mm thick. Specimens of 2×5 mm cross section with 30 mm of gage length for tensile test and 55 × 10 × 10 mm for ASTM standard V-notched Charpy impact test were cut from the sheets along the rolling direction and underwent solid solution treatment by quenching from 1,323 K into water after 1 h of soaking period under Ar gas atmosphere. Tensile tests were performed at 4, 77, and 293 K, respectively, at a strain rate of  $5.5 \times 10^{-4} \text{ s}^{-1}$ . Charpy impact tests were carried out at temperatures ranging from 77 ~ 293 K using V-notch specimens and L–T orientation per ASTM E616. Fracture morphology and microstructure were examined by scanning electron microscope (SEM).

In order to investigate the relationship between fracture and its microstructure, a dual surface observation technique was used. To do this, the fracture surface was first embedded with epoxy resin. Then, the sample underwent grinding, polishing and etching as in a regular metallographic preparation along a plane perpendicular to the fracture surface. The epoxy resin was finally removed by pulling it apart with pliers. In this way, the fracture surface and the etched side surface can be observed simultaneously under microscope.

### Results and discussion

#### Low temperature brittle fracture and three kinds of fracture facets

Figure 1a is the stress–strain curves from the tensile test which shows strength of the steel increases abruptly while ductility and toughness decrease rapidly as temperature is lowered. Figure 1b shows impact energy versus temperature curves for four kinds of austenitic steels including 18Cr–18Mn–0.5N [3, 7], 18Cr–18Mn–0.8N [7], 18Mn–

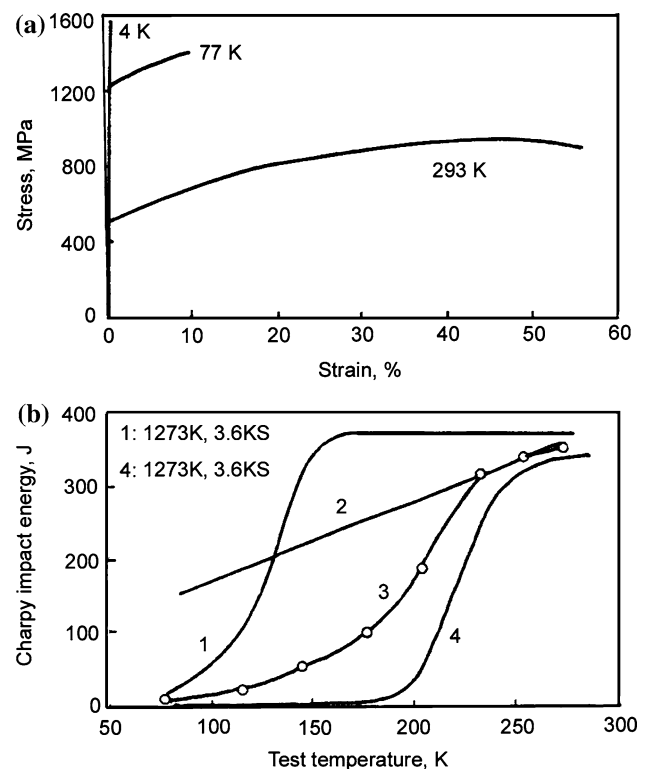
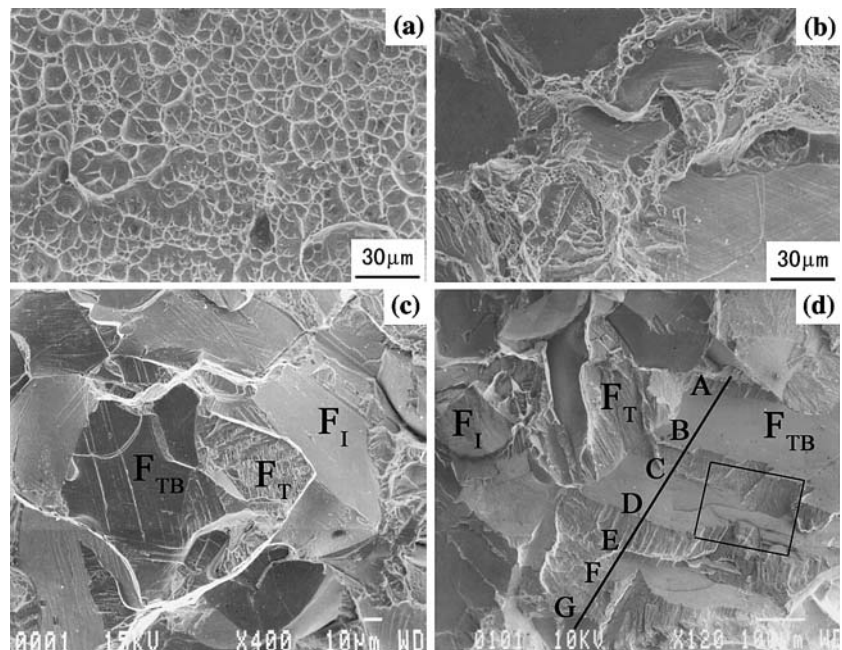


**Fig. 1** (a) Tensile engineering stress–strain curves for high nitrogen austenitic steels and (b) impact energy–temperature curves (1. Fe–18Mn–18Cr–0.5N [3, 7], 2. Fe–18Mn–5Cr–0.5C [3, 7], 3. Fe–18Mn–18Cr–0.7N in the present work, 4. Fe–18Mn–18Cr–0.8N [7], data embedded in the Charpy curve are solution treatment condition for Materials 1 and 4)

5Cr–0.5C [3, 7], and the steel used in this study. It is shown that there is not evident ductile-to-brittle transition for 18Mn–5Cr–0.5C steel that does not contain any nitrogen while high nitrogen austenitic steels exhibit obvious ductile-to-brittle transition. Increasing the nitrogen content raises the ductile-to-brittle transition temperature. For the 18Cr–18Mn–0.7N high nitrogen austenitic steel used in this study, the ductile-to-brittle transition temperature is about 200 K.

Likewise, obvious ductile-to-brittle transition behavior of the tested steel can also be seen from its fracture surface. Fracture at room temperature is totally dimples (Fig. 2a). When temperature drops to 193 K, dimples become smaller and shallower, area percentage of the dimples decreases, and at the same time, smooth fracture facets appear on the fracture (Fig. 2 b). At even lower temperatures, e.g., 77 and 4 K, smoothly flat facets, smoothly curved facets and coarse facets can be seen on the fracture, as indicated by  $F_{TB}$ ,  $F_I$ , and  $F_T$  in Fig. 2c and d, respectively. The size of these facets is about the same as the size of the austenite grains. These facets can also be seen in the previous reports [2, 3], but they were not distinguished in those reports. Among these facets,  $F_{TB}$  possesses all the features of

**Fig. 2** SEM fractographs for specimens (a) impact fractured at 293 K, (b) impact fractured at 193 K, (c) impact fractured at 77 K, and (d) tensile fractured at 4 K ( $F_T$ —transgranular fracture facet,  $F_I$ —intergranular fracture facet,  $F_{TB}$ —annealing twin boundary fracture facet. ABCDEFG—the line along which the specimen was sectioned for dual-surface observation in Fig. 3)



transgranular cleavage-like fracture facet mentioned in the earlier research works [2, 3], i.e., flat, smooth, and no steps and river patterns. As stated above, the present authors have identified by fracture path observation that there are three fracture modes, i.e., annealing twin boundary fracture, intergranular fracture, and transgranular fracture, in low temperature brittle fracture of high nitrogen austenitic steel. Dual-surface observation also exemplified that these three types of fracture modes produce, respectively, smoothly flat facets, smoothly curved facets and coarse facets as designated by  $F_{TB}$ ,  $F_I$ , and  $F_T$  in Fig. 2c and d. More details about the relationship between cracking paths, fracture modes, and fracture appearance can be found in literatures 11–14.

#### Morphological features of transgranular fracture facet

##### *Identification of transgranular fracture facet, intergranular fracture facet, and annealing twin boundary fracture facet*

Since three types of fracture facets are included in the low temperature fracture of high nitrogen austenitic steel, identifying one from the others is not easy. The dual-surface observation proved effective for this purpose, which can be seen from the following example.

The opposite part of the fractured specimen used in Fig. 2d was sectioned perpendicularly to the macrofracture surface along a line parallel with line ABCDEFG and embedded with resin to protect the fracture facets. After the sectioned side surface was abraded, polished, and etched as in a regular metallographic preparation, the final cut along

line ABCDEFG was obtained and the resin was then removed from the specimen. The dual-surface observation of both the fracture surface and the adjacent side surface was then conducted under SEM. The result is shown by an SEM photograph in Fig. 3a. The broken lines A'B'C'D'E'F'G' in Fig. 3a correspond to line ABCDEFG in Fig. 2d. The part above A'B'C'D'E'F'G' is the fracture surface and the part under A'B'C'D'E'F'G' is the microstructure on the side surface where shows an annealing twin microstructure. Here, it can be seen that the smoothly flat facets corresponding to AB, CD, EF were formed from rupture along the annealing twin boundaries and coarse facets corresponding to BC, DE, FG were a result of rupture passing through the grains.

Figure 3b shows an enlarged SEM photograph for the framed area in Fig. 2d. From Fig. 3a it is known that the area indicated by  $F_T$  in Fig. 3b is a transgranular facet corresponding to BC mentioned above, while the area indicated by  $F_{TB}$  in Fig. 3b is an annealing twin boundary facet corresponding to CD mentioned above. The transgranular facet is coarse and uneven, with three sets of parallel step-patterns on it as indicated by A–A, B–B, and C–C. The distance between two steps ranges from about 1 to 8  $\mu\text{m}$ . Obviously, the transgranular facet is different from annealing twin boundary facet because the former displays step-patterns and is very coarse while the latter very smooth and flat. Detailed discussion on intergranular facet will not be given in this study. According to Refs. [11] and [12], however, intergranular facet is also very smooth, which is similar to annealing twin boundary facet, and is completely different from the transgranular facet.



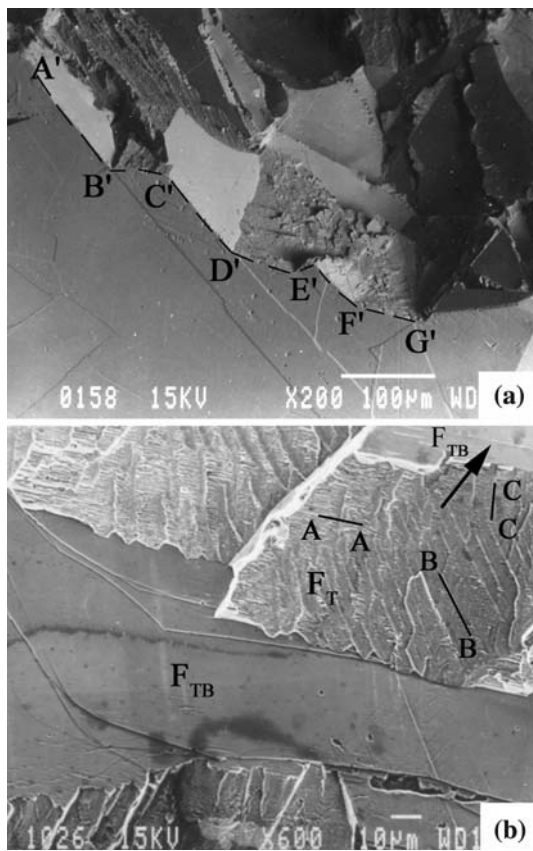


**Fig. 3** SEM micrographs of fracture appearance and microstructure for a specimen tensile fractured at 4 K: (a) SEM micrograph of dual-surface observation of fracture surface and microstructure on the side surface, (b) enlarged micrograph of framed area in Fig. 2(d) (A'B'C'D'E'F'G'—dashed lines correspond to ABCDEFG in Fig. 2(d))

Based on the differences mentioned above in transgranular facet, annealing twin boundary facet, and intergranular facet, the transgranular facet can be identified from the other two facets in low temperature brittle fracture of high nitrogen austenitic steel. Figure 4 shows three SEM micrographs of some transgranular facets for the steel used in this study fractured at 77 and 4 K. Besides being very coarse compared with annealing twin boundary facet (including intergranular facet), the other two typical features of the transgranular facet are: (1) there are steps and river patterns on the facet, (2) the facet is covered by fine pits.

*Steps and river patterns*

Similar to the steps and river patterns on cleavage fracture for BCC metals, there are steps and river patterns on the transgranular facet of low temperature brittle fracture for FCC high nitrogen austenitic steel as shown in Fig. 4a and b. Since crack in low temperature brittle fracture for high nitrogen austenitic steel would propagate either through grain boundary (including annealing twin boundary) or

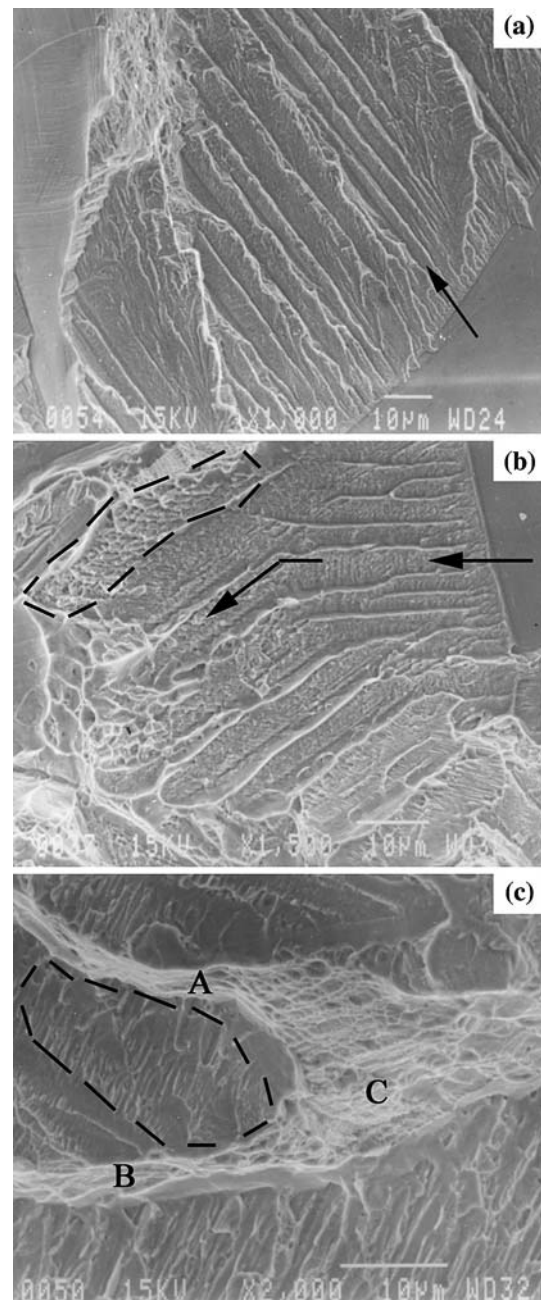


**Fig. 4** SEM fractographs of transgranular fracture facets: (a) enlarged micrograph of the fracture facet indicated by F<sub>T</sub> in Fig. 2(d), (b) and (c) for specimens fractured at 77 K

through trans-grain, and the intergranular crack is easier to form than the transgranular crack [11, 12], it is often the case that a crack propagates preferably along grain boundaries and, when coming across another grain, induces a transgranular crack. This results in a sharp facet change from smooth to coarse, forming large amount of steps and river patterns. The morphological change here is more obvious than the one occurs with cleavage fracture in BCC metals.

During the procedure when a crack is propagating from one side of a grain to the other side of the grain, the steps and river patterns on the facet are also changing. The general rule goes this way: upon the beginning of transgranular cracking, many smaller steps form and then join together to form higher but less steps, and on some area river patterns take form; next, as the cracking advances, the steps become even higher, and passing through the grain to the other side of the grain. From the transgranular facets in Fig. 4(a) and (b), this changing procedure can obviously be seen. According to the river pattern direction, one can identify cracking direction of the transgranular fracture in the micro area, as shown with arrows on the figures.

Careful observation indicates that steps and river patterns on the transgranular facet are in group and are basically straight, flat, and parallel in each individual group, showing crystallographic characteristics. In Fig. 4a, one group of parallel steps traverse through a grain from one side to the other. In Fig. 4b, transgranular fracture starts in a group of smaller parallel steps, and then turns its fracture direction in another group of larger parallel steps.

Comparing the facet from 4 K in Fig. 4a with those from 77 K in Fig. 4b and c, it can be seen that temperature has some effect to a certain extent on the plastic deformation during transgranular fracture and the facet morphology. Figure 4a is an enlarged SEM photograph for the transgranular facet denoted by  $F_T$  in Fig. 2d. There is little sign of tear deformation during transgranular fracture in the facet from 4 K. Figure 4b shows a facet from 77 K. Its surface is rougher which means more tear deformation took place in the process of transgranular fracture. On the facet from 77 K, tear ridges can sometimes be observed as denoted by A, B and C in Fig. 4c. It is believed that this kind of ridge is a consequence of joint of transgranular cracks of different heights, resulting in much more plastic deformation.

#### Pits

On all of the transgranular facets, fine pits can be seen (e.g., the areas surrounded by dash lines in Fig. 4b and c). Their size is around 1  $\mu\text{m}$  or even tiny, distributing uniformly among steps and river patterns. Though small, they often appear in certain shapes and directions. Specifically, the elongated pits in Fig. 4c parallel each other, showing definite crystallographic features. Along the propagating direction in transgranular fracture, which can be obtained from the river pattern direction, it can be seen that, more the crack traverses a grain from one side to another, the larger are the pits, suggesting that plastic deformation is increasing at the same time. Once again, the pits on the 77 K facet are more obvious than those on the 4 K facet, indicating less plastic deformation in transgranular fracture at 4 K.

#### Formation of transgranular facet

Study on the fracture of high nitrogen austenitic steel shows that large amount of deformation structures form even if in brittle fracture under low temperature. These deformation structures include planar dislocation arrays [3, 15], deformation twins and stacking faults, etc [8]. Study also indicates that these deformation structures are formed on  $\{111\}$  planes in FCC crystals [3, 8]. Because the low temperature deformation structures are planar for high nitrogen austenitic steels, they are termed planar deformation structures [7, 15].

As discussed above, steps and river patterns on the low temperature transgranular facets in high nitrogen austenitic steels exhibit strict crystallographic characteristics. From the facet observation, it is revealed that step patterns on the transgranular facet are parallel to deformation structures. For example, in the SEM photomicrograph of a fracture at 4 K as shown in Fig. 3b, the steps in A–A direction on the transgranular facet are parallel to the deformation structures as the arrow indicates on the annealing twin boundary facet. Since the deformation structures are parallel to  $\{111\}$  planes, steps and river patterns on the transgranular facet are parallel to  $\{111\}$  planes.

Figure 5 is a photomicrograph of the side surface near a fracture from 77 K. There is a small crack on the grain boundary as denoted by Arrow A. Within the grain, there are a great number of deformation structures along  $\{111\}$  planes, but the deformation does not distribute evenly. Deformation structures moving along different slip planes intersect each other, leaving microcracks at the intersecting points of severe deformation structures as denoted by Arrow B.

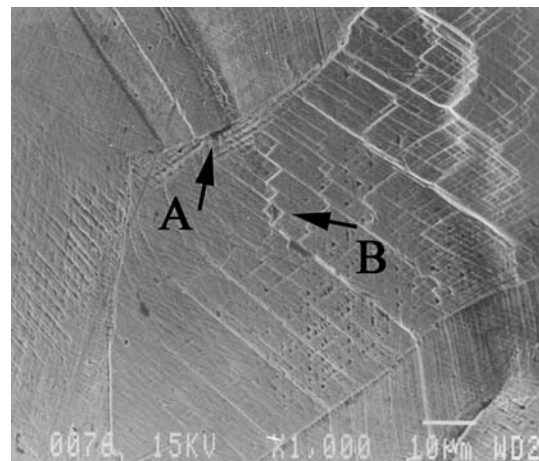


**Fig. 5** SEM image showing microstructure and microcracks induced during impact fracture in the vicinity of the fracture surface of specimen ruptured at 77 K

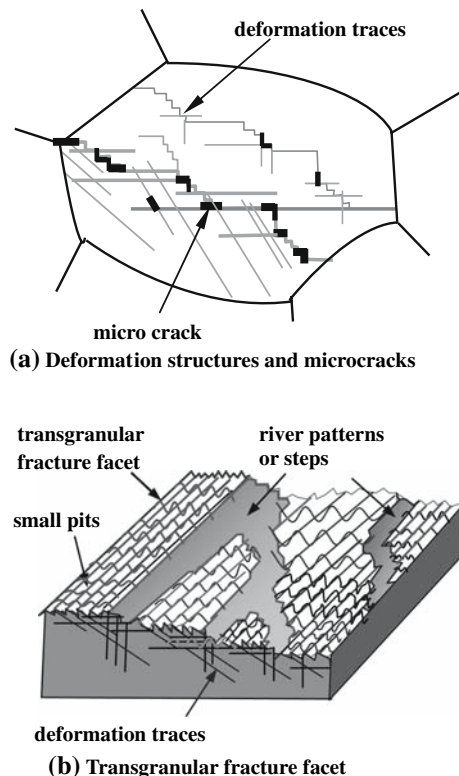


**Fig. 6** Schematic illustration of the transgranular fracture

Based on this observation and morphological features of the facet, a mechanism of formation of transgranular facet is proposed as schematically illustrated in Fig. 6. Subjected to an externally applied stress, a large amount of deformation structures are formed along  $\{111\}$  planes. Deformation structures on different  $\{111\}$  planes intersect each other and form microcracks (Fig. 6a). These microcracks then coalesce to form cracks that continue to propagate, leading ultimately to the transgranular fracture. Cracks propagating on the parallel  $\{111\}$  planes at a wider distance coalesce to form parallel steps and river patterns, while those at shorter distances in between take on the form of fine pits by propagation and coalescence (Fig. 6b).

## Conclusion

- (1) There are three types of fracture modes in low temperature brittle fracture for 18Cr–18Mn–0.7N high

nitrogen austenitic steel: annealing twin boundary fracture, intergranular fracture and transgranular fracture. The transgranular fracture facets are coarse and uneven. On these facets, there are plenty of uniformly distributed fine pits of similar shape, and parallel steps and river patterns that are in correspondence with deformation structures on  $\{111\}$  planes and show distinct crystallographic features.

- (2) A large number of deformation structures form along  $\{111\}$  planes during low temperature brittle fracture of high nitrogen austenitic steel. Intersections of deformation structures on different  $\{111\}$  planes cause stress concentration and originate microcracks, which propagate and coalesce to form transgranular fracture. Coalescence of cracks propagating on parallel  $\{111\}$  planes of different distances within a grain induces steps, river patterns, and pits that show definite crystallographic characteristics. As the transgranular cracking propagates, steps, river patterns and pits become coarser.

**Acknowledgement** The authors thank the Japan Steel Works Ltd. for supplying the experimental steel.

## References

1. ASM Handbook Committee (1987) In: ASM handbook, vol. 12. Fractography. ASM International, USA, p 12
2. Tobler RL, Meyn D (1988) Metal Trans A 19A:1626
3. Tomota Y, Endo S (1990) Iron Steel Inst Jpn Int 30:656
4. Ishizaka J, Orita K, Terao K (1992) Tetsu-to-Hagané 78:1846
5. Tomota Y (1994) Tetsu-to-Hagané 80:N538
6. Tomota Y, Nakano J, Xia J, Inoue K (1998) Acta Mater 46:3099
7. Tomota Y, Xia Y, Inoue K (1998) Acta Mater 46:1577
8. Chen KM, Dai QX (1998) J Iron Steel Res 10(1):38 (in Chinese)
9. Wang AD, Dai QX, Cheng XN (2000) J Jiangsu Univ Sci Tech (Natural Sci) 5:59 (in Chinese)
10. Yuan ZZ, Dai QX, Cheng XN, Chen KM, Xu WW (2004) J Jiangsu Univ Sci Tech (Natural Sci) 25:247 (in Chinese)
11. Liu SC, Hashida T, Takahashi H, Kuwano H, Hamaguchi Y (1998) Metal Trans A 29A:791
12. Liu SC, Liu DY, Dai YK (2002) Acta Metal Sinica 38:1042 (in Chinese)
13. Liu SY, Liu SC, Liu DY (2004) J Mater Sci 39:2841
14. Liu SC, Liu DY, Chen RS, Dai YK (2005) Trans Mater Heat Treat 4:33 (in Chinese)
15. Kubota S, Xia Y, Tomota Y (1998) Iron Steel Inst Jpn Int 38:474